Anal. Chem. **2010,** *82,* 2448–2455

Low-Potential Detection of Endogenous and Physiological Uric Acid at Uricase−Thionine−Single-Walled Carbon Nanotube Modified Electrodes

Dongxiao Chen,[†] Qian Wang,[†] Juan Jin,[†] Ping Wu,[†] Hui Wang,[‡] Shuqin Yu,[‡] Hui Zhang,*[,†] and Chenxin Cai*[,†]

Jiangsu Key Laboratory of Biofunctional Materials, Laboratory of Electrochemistry, College of Chemistry and Environmental Science, and College of Life Science, Nanjing Normal University, Nanjing 210046, People's Republic of China

This work develops and validates an electrochemical approach for uric acid (UA) determinations in both endogenous (cell lysate) and physiological (serum) samples. This approach is based on the electrocatalytic reduction of enzymatically generated H_2O_2 at the biosensor of uricase−thionine−single-walled carbon nanotube/glassy carbon (UOx−Th−SWNTs/GC) with the use of Th−SWNTs nanostructure as a mediator and an enzyme immobilization matrix. The biosensor, which was fabricated by immobilizing UOx on the surface of Th−SWNTs, exhibited a rapid response (ca. 2 s), a low detection limit (0.5 ± 0.05 μM), a wide linear range (2 μM to 2 mM), high sensitivity ($\sim$90 μA mM^{-1} cm^{-2}), as well as good stability and repeatability. In addition, the common interfering species, such as ascorbic acid, 3,4-dihydroxyphenylacetic acid, 4-acetamidophenol, etc., did not cause any interference due to the use of a low operating potential (−400 mV vs saturated calomel electrode). Therefore, this work has demonstrated a simple and effective sensing platform for selective detection of UA in the physiological levels. In particular, the developed approach could be very important and useful to determine the relative role of endogenous and physiological UA in various conditions such as hypertension and cardiovascular disease.

Uric acid (UA) is the main end-product of endogenous and dietary purine derivatives in human metabolism.[1] It is generated by the xanthine oxidase-catalyzed conversion of xanthine and hypoxanthine. Its normal level in serum ranges from 0.3 to 0.5 mM and in urinary excretion is typically 1.4−4.4 mM.[2] The alterations of UA concentration in body fluids may cause lots of diseases and pathological disorders including gout,[3] arthritis,[4] kidney disease,[5] cardiovascular disease,[6] neurological diseases,[7] etc. Therefore, it is an important marker molecule for diagnosis and treatment of these disorders. Reliable and simple approaches for routinely detection of UA are required in clinical laboratory. Moreover, UA could play as an antioxidant in several tissues to protect body against oxidative damage caused by ROS (reactive oxygen species).[8] Recent studies suggest that soluble UA can enter cells via specific transporters where it can induce proinflammatory and prooxidative effects.[9,10] Thus, the intracellular UA concentration has been a key in the mediation of its cellular effects,[5,11−15] and its measurement is important in evaluating the oxidative damage caused by ROS. Therefore, the determination of concentration of the intracellular and extracellular UA could lead to a better understanding of the clinical consequence of elevated UA as well assist in studies designed to test the biological effect of UA in cells.

Various techniques have been developed for analysis UA in its biological environment, including electrochemical methods,[16−19]

* To whom correspondence should be addressed. E-mail: zhangh@njnu.edu.cn (H.Z.); cxcai@njnu.edu.cn (C.C.).

† College of Chemistry and Environmental Science.

‡ College of Life Science.

(1) Watanabe, S.; Kimura, Y.; Shindo, K.; Fukui, T. *J. Health Sci.* **2006**, *52*, 738–742.

(2) Ames, R. B.; Cathcart, R.; Schwiers, E.; Hochstein, P. *Proc. Natl. Acad. Sci. U.S.A.* **1981**, *78*, 6858–6862.

(3) Chu, Q. C.; Lin, M.; Geng, C. H.; Ye, J. N. *Chromatographia* **2007**, *65*, 179–184.

(4) Wortmann, R. L. Disorders of purine pyrimidine metabolism. In *Harrison's Principles of Internal Medicine*, 15th ed.; Braunwald, E., Fauci, A. S., Kasper, D. L., Hauser, S. L., Longo, D. L., Jameson, J. L., Eds.; McGraw-Hill: New York, 2001; pp 2268−2273.

(5) Khosla, U. M.; Zharikov, S.; Finch, J. L.; Nakagawa, T.; Roncal, C.; Mu, W.; Krotova, K.; Block, E. R.; Prabhakar, S.; Johnson, R. J. *Kidney Int.* **2005**, *67*, 1739–1742.

(6) Baker, J. F.; Krishnan, E.; Chen, L.; Schumacher, H. R. *Am. J. Med.* **2005**, *118*, 816–826.

(7) Moallem, H. J.; Taningo, G.; Jiang, C. K.; Hishhorn, R.; Fikrig, S. *Clin. Immunol.* **2002**, *105*, 75–80.

(8) Moora, E.; Kohen, R.; Reiter, R. J.; Shohami, E. *Neurosci. Lett.* **2001**, *316*, 169–172.

(9) Burkhardt, S.; Reiter, R. J.; Tan, D. X.; Hardeland, R.; Cabrera, J.; Karbownik, M. *Int. J. Biochem. Cell Biol.* **2001**, *33*, 775–783.

(10) Nieto, F. J.; Iribarren, C.; Gross, M. D.; Comstock, G. W.; Cutler, R. G. *Atherosclerosis* **2000**, *148*, 131–139.

(11) Kanellis, J.; Watanabe, S.; Li, J. H.; Kang, D. H.; Li, P.; Nakagawa, T.; Wamsley, A.; Sheikh-Hamad, D.; Lan, H. Y.; Feng, L.; Johnson, R. J. *Hypertension* **2003**, *41*, 1287–1293.

(12) Kang, D. H.; Park, S. K.; Lee, I. K.; Johnson, R. J. *J. Am. Soc. Nephrol.* **2005**, *16*, 3553–3562.

(13) Corry, D. B.; Eslami, P.; Yamamoto, K.; Nyby, M. D.; Makino, H.; Tuck, M. L. *J. Hypertens.* **2008**, *26*, 269–275.

(14) Segal, M. S.; Gollub, E.; Johnson, R. J. *Eur. J. Nutr.* **2007**, *46*, 406–417.

(15) Sautin, Y. Y.; Nakagawa, T.; Zharikov, S.; Johnson, R. J. *Am. J. Physiol. Cell Physiol.* **2007**, *293*, C584–C596.

(16) Behera, S.; Raj, C. R. *Biosens. Bioelectron.* **2007**, *23*, 556–561.

10.1021/ac9028246
Published on Web 02/17/2010

chemiluminescence,[20−23] fluorescence,[24] chromatography,[3,25−28] etc. Among those methods, the electrochemical approach has attracted significant attention and is a promising method because of their high sensitivity, low cost, rapid response, compatibility for miniaturization, low manpower requirements, and compatibility with microfabrication technology. The assay based on the direct electrochemical oxidation of UA are usually affected by the presence of other oxidizable species such as ascorbic acid (AA), dopamine (DA), etc., in biological samples.[29,30] There were a lot of papers published on the determination of the concentration of UA in the brain extracellular fluid (ECF) based on the direct electrochemical oxidation of UA at carbon paste and electrochemically treated carbon fiber electrodes,[31−36] which are the two electrode materials most widely used to detect UA in ECF. The electrooxidation of UA is relatively well-behaved at both surfaces of the two types of electrodes with peak potentials in the range of 250−350 mV, depending on the reference electrode. However, the coexisted 5-hydroxytryptamine (5-HT) and 5-hydroxyindoleacetic acid (5-HIAA) have voltammetric peak potentials very similar to UA, although not identical.[31,32,34,35,37] As a result, voltammograms recorded in ECF consist of a single peak, and only very complicated deconvolution analysis can separate the three signals under some conditions.[37] These lead to the development of a uricase-based electrochemical method since enzymes have a unique ability of molecular recognition, and consequently enzyme-based assay is highly selective and sensitive.

Uricase (UOx) catalyzes the oxidation of UA to allantoin in the presence of oxygen, producing CO_2 and H_2O_2 simultaneously. Quantification of UA is achieved by measuring the concentration decrease of the dissolved oxygen in the system[38−40] or determining the amount of the enzymatically generated H_2O_2.[16,17,41] Because the linear range of the assay based on O_2 consumption is usually narrow (between 0.1 and 0.5 μM),[42] the method based on the determination of H_2O_2 has received considerable interest. However, the oxidation of H_2O_2 usually requires a relatively high positive potential (usually over +0.6 V vs SCE). Many other electroactive species usually coexisting in the biological fluids can also be oxidized at the high potential, and their electrochemical signals thus severely affect the selectivity of the assay. Moreover, UA itself is oxidized at the electrode's surface at such a high potential. Therefore, interference elimination represents a main task to be solved for this type of biosensor. The interference can be partially overcome by coating the biosensor with a membrane impermeable to interfering species[43] or oxidizing the interfering species before they reach the biosensor.[44] However, coating with polymeric films leads to lower signals and longer response time due to the additional diffusion barrier, whereas using electrochemical preoxidation displays a risk of oxidizing the substrate of interest. To eliminate this risk, the oxidation of the interfering species can be accomplished by enzymatic preoxidation,[45] which is achieved either by incorporating specific enzymes in the sensor configuration or immobilizing them in reactors, thus complicating the biosensor fabrication procedures.

Alternatively, the enzymatically generated H_2O_2 can be monitored based on its reduction because the electrochemical reduction of H_2O_2 that occurred at a relatively negative potential does not give rise to the interference from those interfering species. Behera and Raj reported a UA biosensor based on the reduction of H_2O_2 at the gold electrode by covalently coimmobilizing microperoxidase-11 (MPx-11) and UOx on the mixed self-assembled monolayer of 2-(2-mercaptoethylpyrazine) (PET) and 4,4′-dithiodibutyltyric acid (DTB).[16] However, the procedures of biosensor fabrication are very complicated. This work reports a UOx-based UA biosensor based on the reduction of H_2O_2 with the use of thionine−single-walled carbon nanotube (Th−SWNTs) nanostructures as mediator and immobilization matrix. The preparation and characteristics of the novel UA biosensor are presented. It is demonstrated that Th−SWNTs possess the properties of individual components with a synergistic effect toward the reduction of H_2O_2. This biosensor exhibits ease of fabrication, good performance, fast response, nice stability and reproducibility, and low detection limit. Moreover, the developed biosensor can be used for UA measurements in both endogenous (cell lysate) and the physiological (serum) samples. In particular, the developed

(17) Moraes, M. L.; Rodrigues Filho, U. P.; Oliveira, O. N., Jr.; Ferreira, M. *J. Solid State Electrochem.* **2007**, *11*, 1489–1495.
(18) Liao, C. W.; Chou, J. C.; Sun, T. P.; Hsiung, S. K.; Hsieh, J. H. *IEEE Trans. Biomed. Eng.* **2006**, *53*, 1401–1408.
(19) Prasad, K. S.; Muthuraman, G.; Zen, J. M. *Electrochem. Commun.* **2008**, *10*, 559–563.
(20) He, D.; Zhang, Z.; Huang, Y.; Hu, Y.; Zhou, H.; Chen, D. *Luminescence* **2005**, *20*, 271–275.
(21) Lin, Z.; Chen, Z.; Liu, Y.; Wang, J.; Chen, G. *Analyst* **2008**, *133*, 797–801.
(22) Poole, R. A.; Kielar, F.; Richardson, S. L.; Stenso, P. A.; Parker, D. *Chem. Commun.* **2006**, 4084–4086.
(23) Wu, F.; Huang, Y.; Li, Q. *Anal. Chim. Acta* **2005**, *536*, 107–113.
(24) Galban, J.; Andreu, Y.; Almenara, M. J.; de Marcos, S.; Castillo, J. R. *Talanta* **2001**, *54*, 847–854.
(25) Kim, K. M.; Henderson, G. N.; Ouyang, X.; Frye, R. F.; Sautin, Y. Y.; Feig, D. I.; Johnson, R. J. *J. Chromatogr., B* **2009**, *877*, 2032–2038.
(26) Cooper, N.; Khoseravan, R.; Erdmann, C.; Fiene, J.; Lee, J. W. *J. Chromatogr., B* **2006**, *837*, 1–10.
(27) Czauderna, M.; Kowalczyk, J. *J. Chromatogr., B* **1997**, *704*, 89–98.
(28) Cirillo, P.; Gersch, M. S.; Mu, W.; Scherer, P. M.; Kim, K. M.; Gesualdo, L.; Henderson, G. N.; Johnson, R. J.; Sautin, Y. Y. *J. Am. Soc. Nephrol.* **2009**, *20*, 545–553.
(29) Hasoò, S.; Vetterl, V.; Jelen, F.; Fojta, M. *Electrochim. Acta* **2009**, *54*, 1864–1873.
(30) Zhang, L.; Zhang, C.; Lian, J. *Biosens. Bioelectron.* **2008**, *24*, 690–695.
(31) O'Neill, R. D.; Lowry, J. P. *Behav. Brain Res.* **1995**, *71*, 33–49.
(32) O'Neill, R. D.; Gonzalez-Mora, J.-L.; Boutelle, M. G.; Ormonde, D. E.; Lowly, J. P.; Duff, A.; Fumero, B.; Fillenz, M.; Mas, M. *J. Neurochem.* **1991**, *57*, 22–29.
(33) O'Neill, R. D. *Analyst* **1994**, *119*, 767–779.
(34) Crespi, F.; Sharp, T.; Maidment, N.; Marsden, C. A. *Neurosci. Lett.* **1983**, *43*, 203–207.
(35) Cespuglio, R.; Sarda, N.; Gharib, A.; Faradji, H.; Chastrette, N. *Exp. Brain Res.* **1986**, *64*, 589–595.
(36) O'Neill, R. D.; Fillenz, M.; Grunewald, R. A.; Bloomfield, M. R.; Albery, W. J.; Jamieson, C. M.; Williams, J. H.; Gray, J. A. *Neurosci. Lett.* **1984**, *45*, 39–46.
(37) Guadalupe, T.; Gonzalez-Mora, J.-L.; Fumero, B.; Mas, M. *J. Neurosci. Methods* **1992**, *45*, 159–164.
(38) Arora, J.; Nandwani, S.; Bhambi, M.; Pundir, C. S. *Anal. Chim. Acta* **2009**, *647*, 195–201.
(39) Wang, X.; Hagiwara, T.; Uchiyama, S. *Anal. Chim. Acta* **2007**, *587*, 41–46.
(40) Zhang, Y.; Wen, G.; Zhou, Y.; Shuang, S.; Dong, C.; Choi, M. M. F. *Biosens. Bioelectron.* **2007**, *22*, 1791–1797.
(41) Arora, K.; Sumana, G.; Saxena, V.; Gupta, R. K.; Gupta, S. K.; Yakhmi, J. V.; Pandey, M. K.; Chand, S.; Malhotra, B. D. *Anal. Chim. Acta* **2007**, *594*, 17–23.
(42) Zhang, F.; Li, C.; Li, X.; Wang, X.; Wan, Q.; Xian, Y.; Jin, L.; Yamanmoto, K. *Talanta* **2006**, *68*, 1353–1358.
(43) Hoshi, T.; Saiki, H.; Anzai, J. I. *Talanta* **2003**, *61*, 363–368.
(44) Luo, Y. C.; Do, J. S.; Liu, C. C. *Biosens. Bioelectron.* **2006**, *22*, 482–488.
(45) Miland, E.; Ordieres, A. J. M.; Blanco, P. T.; Smyth, M. R.; Fágáin, C. Ó. *Talanta* **1996**, *43*, 785–796.

approach could be very important as there is increasing evidence that intracellular UA may have a role in hypertension, insulin resistance, and vascular disease. Our goal is not only to design a novel biosensing platform but also to present a new approach for determination of UA, which has potential utility to bioelectroanalytical chemistry, cellular biology, pathophysiology, etc.

EXPERIMENTAL SECTION

Chemicals. UOx (EC 1.7.3.3, from *Bacillus fastidiosus*, lyophilized powder, approximately 14.5 units/mg, Fluka), glucose, 3,4-dihydroxyphenylacetic acid (DOPAC), AA, UA, 4-acetamidophenol (AP), D-fructose, sodium dodecylbenzene sulfonate (SDBS), and thionine (in the form of chloride) were used as received. SWNTs (<2 nm in diameter, Shenzhen Nanotech Port, Shenzhen, China) were purified following the reported method.[46] All other chemicals were of analytical grade. All solutions were prepared with double-distilled water. Solutions of H_2O_2 were freshly diluted from the 30% solution, and their concentrations were determined using a standard $KMnO_4$ solution. A 0.1 M phosphate buffer solution (PBS, pH 7.4) was employed as the supporting electrolyte. A stock UA solution was prepared in 0.3 M NaOH at a concentration of 10 mM and then diluted to 1 mM in PBS, with pH adjusted to 7.4 using 1 M HCl.

Preparation of the Thionine−Single-Walled Carbon Nanotube/Glassy Carbon Electrode and Immobilization of UOx. Thionine and UOx were assembled on the surface of SWNTs by taking advantage of the electrostatic interaction of these components. Several experimental parameters were optimized to obtain the best voltammetric response. Typically, 1 mg of SWNTs was dispersed in 1 mL of SDBS aqueous solution (0.5 wt %) with the aid of ultrasonication forming 1 mg mL^{-1} SWNTs suspension. When SWNTs were sonicated and incubated in the solution, the SDBS molecules were adsorbed on the surface of SWNTs through hydrophobic interactions creating a distribution of negative charges on SWNTs surface. These charges prevent the SWNTs from aggregation and induce their suspension in water. Afterward, the SDBS-coated SWNTs were collected by centrifugation at 18 000 rpm for 30 min. The supernatant was removed, and the SWNTs (hereafter, unless otherwise specified, the SWNTs are referred to SDBS-coated SWNTs) were thoroughly washed at least thrice with water to remove the loosely adsorbed SDBS. To fabricate the SWNT/GC electrode, 2 mg of SWNTs were dispersed in 1 mL of water to give a 2 mg mL^{-1} SWNTs suspension. Then, 2 μL of the suspension was cast onto the surface of pretreated glassy carbon electrode (GC, 3 mm in diameter, CH Instruments) with a microsyringe and the solvent was allowed to evaporate at ambient temperature before use.

To assemble thionine and UOx, the SWNT/GC electrode was first immersed in thionine solution (1 mM) for 30 min since the voltammetric results demonstrated that the amount of thionine on the surface of the electrode tends to be saturated after that time. The resulted Th−SWNT/GC electrode was thoroughly rinsed with water. Then, the electrode was incubated in UOx solution (2.5 mg mL^{-1} in PBS solution, pH 7.4) at 4 °C for 1 h.

Scheme 1. Schematic Illustration of the Dimension and the Structure of the Active Component of the UOx−Th−SWNT/GC Electrode

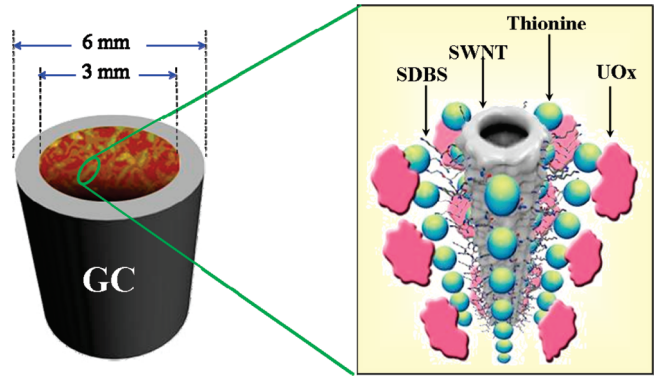

UOx is negatively charged in pH 7.4 PBS because the isoelectric point of the enzyme is ~5.4.[17] Therefore, the enzyme is easily assembled on the surface of the positively charged Th−SWNT/GC electrode forming the UOx−Th−SWNT/GC electrode (the dimension and the structure of the active component of the electrode are schematically illustrated in Scheme 1). After being thoroughly rinsed with PBS, the electrode was ready to be used for catalytic oxidation of UA. The electrode was stored at 4 °C when not in use. For comparison, the UOx/GC, UOx−Th/GC, and UOx−SWNT/GC electrodes were also prepared using similar procedures.

Cell Culture and Cell Lysate Preparation. The concentration of UA in human embryonic kidney 293A cells (HEK 293A) was determined using the developed electrode. Cells were grown at 37 °C in DMEM (Dulbecco's modified Eagle medium) supplemented with 10% (v/v) fetal bovine serum (FBS), 100 U mL^{-1} penicillin, and 100 μg mL^{-1} streptomycin in a 5% CO_2 environment.[47] After cells grew at 90% confluence, cells were then washed with PBS and the cell number was calculated by hemocytometer. Cells were lysed with 0.3 M KOH, and then the lysate was sonicated. The samples were centrifuged at 18 000 rpm for 30 min, and the supernatant was filtered through a 0.22 μm Nylon filter. The concentration of UA in the filtrates was measured by an electrochemical method using the UOx−Th−SWNT/GC electrode.

To study the effect of D-fructose on the UA production in HEK 293A cells, 5 mM D-fructose was added to cells to induce UA generation. After treatment of the cells for various times, the cells were lysed with 0.3 M KOH, centrifuged at 16 000 rpm for 30 min, and the supernatant was filtered with a Nylon filter. The concentration of UA was analyzed.

Apparatus and Procedures. Atomic force microscopic (AFM) images were recorded with a Nanoscope IIIa scanning probe microscope (Digital Instruments, U.S.A.) using a tapping mode. The FT-IR spectrum was recorded on a Nexus 670 FT-IR spectrophotometer (Nicolet Instruments) using a KBr disk at a resolution of 4 cm^{-1}.

The electrochemical experiments were carried out with a CHI 660B electrochemical workstation (CH Instruments). A two-compartment three-electrode cell with the sample volume of 10 mL was employed. A coiled Pt wire and a saturated calomel

(46) Tohji, K.; Goto, T.; Takahashi, H.; Shinoda, Y.; Shimizu, N.; Jeyadevan, B.; Matsuoka, I. *Nature* **1996**, *383*, 679.

(47) Hooper, C.; Killick, R.; Tavassoli, M.; Melino, G.; Lovestone, S. *Neurosci. Lett.* **2006**, *401*, 30–34.

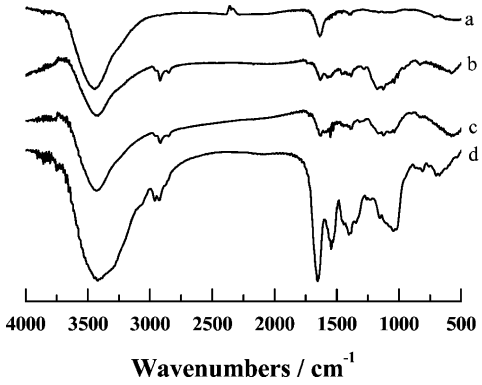

Figure 1. FT-IR spectra of the SWNTs (a), SWNTs adsorbed with SDBS (b), Th−SWNTs (c), and UOx−Th−SWNTs (d).

electrode (SCE) were used as the counter electrode and the reference electrode, respectively. Amperometric measurements were performed under an applied potential of −400 mV. The solution was continuously stirred using a magnetic bar at a speed of 250 rpm. The response current was taken as the change between the steady-state and background currents. All electrochemical experiments were performed at the temperature of 37 ± 1 °C.

RESULTS AND DISCUSSION

Characterization. The SWNTs consist of seamlessly rolled-up graphene sheets, exhibit a special sidewall curvature, and possess a π-conjugative structure with a highly hydrophobic surface. These unique properties essentially allow SWNTs to interact with many surfactant molecules through hydrophobic interactions, thus significantly improving the dispersity of SWNTs in water. When SWNTs were sonicated with SDBS solution, a layer of negative charges was created on the surface of the SWNTs via adsorption of the surfactant molecules. Therefore, positively charged thionine and negatively charged UOx (at pH 7.4) could be assembled on the surface of SWNTs in turn based on electrostatic interaction. Those assembly processes were characterized by FT-IR spectroscopy.

As shown in Figure 1a, for purified SWNTs, the characteristic vibration modes of carbonyl group (~1640 cm^{-1}) and hydroxyl group (~3450 cm^{-1}) are obvious, demonstrating that SWNTs have been functionalized with carboxylic and carboxylate groups after treatment.[48] The adsorption of SDBS on the surface of SWNTs results in the characteristic vibration of $-CH_3$ and $-CH_2-$ (~2850 and ~2920 cm^{-1}) in the IR spectrum (Figure 1b). The peaks at ~1180 and 1040 cm^{-1} can be assigned to the $-SO_3$ group antisymmetric and symmetric vibration adsorption, respectively.[49] Peaks at ~1130 and 1010 cm^{-1} can be assigned to the in-plane skeleton vibration and in-plane bending vibration of the benzene ring, respectively. These results indicate that SDBS has been effectively assembled on the surface of SWNTs. After the assembly of thionine, several new peaks are found at ~1565, 1550, 1530, 1510, 1445, 1478, 1495, 1460, and 1313 cm^{-1}, respectively (Figure 1c). These peaks are the characteristic IR features of thionine,[50] indicating that thionine has been effectively assembled on the surface of SWNTs. The demonstration of amide I (1650 cm^{-1}) and amide II (1550 cm^{-1})[51] in the FT-IR spectrum of UOx−Th−SWNTs (Figure 1d) indicates that UOx has been successfully immobilized on the SWNTs via SDBS and thionine.

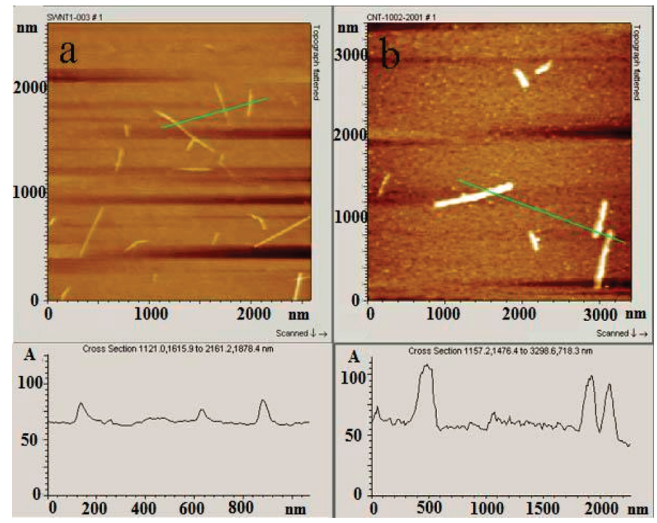

Figure 2. Typical AFM images and the corresponding sectional analysis of Th−SWNTs (a) and UOx−Th−SWNTs (b).

The assembly of UOx on the Th−SWNTs surface is further confirmed by the AFM images (Figure 2). The image of Figure 2a and the corresponding sectional analysis demonstrate that the height of Th−SWNTs is about 2 nm. The image also shows that the Th−SWNTs distribute separately on the surface of the electrode without forming small bundles or entangling each other (Figure 2a), indicating that the nanostructure has a good dispersive ability in aqueous solution. The uniform nanostructure can significantly increase the effective surface of the electrode for loading of biomolecules and accelerating the rate of electron transfer. After UOx was assembled on the surface of the Th−SWNTs, some small and uniformly distributed island-like nanostructures appear (Figure 2b). These nanostructures are the aggregates of UOx molecules, indicating that the enzyme has been effectively immobilized on the surface of Th−SWNTs. Moreover, the size of UOx−Th−SWNTs has a significant increase compared with that of Th−SWNTs (4−5 nm for UOx−Th−SWNTs, see the AFM image in Figure 2b and the corresponding sectional analysis), further indicating the formation of UOx−Th−SWNTs. The morphology of UOx−Th−SWNTs on the electrode surface possesses the similar structure to that of Th−SWNTs. Such a structure is expected to be very attractive for the detection of substrates because each of the UOx−Th−SWNTs is fully and easily accessible to substrates and, therefore, can be used as an electrochemical sensing unit, yielding a high ratio of signal to noise for electrochemical determination.

Electrochemical Reduction of H_2O_2 at the Th−SWNT/GC Electrode. No electrochemical reaction occurred at the SWNT/GC electrode in the N_2-saturated PBS (pH 7.4) in the

(48) Lim, J. K.; Yun, W. S.; Yoon, M. H.; Lee, S. K.; Kim, C. H.; Kim, K.; Kim, S. K. *Synth. Met.* **2003**, *139*, 521–527.
(49) Yang, J. C.; Jablonsky, M. J.; Mays, J. W. *Polymer* **2002**, *43*, 5125–5132.
(50) Jeykumari, D. R. S.; Ramaprabhu, S.; Narayanan, S. S. *Carbon* **2007**, *45*, 1340–1353.
(51) Niwa, K.; Furukawa, M.; Niki, K. *J. Electroanal. Chem.* **1988**, *245*, 275–285.

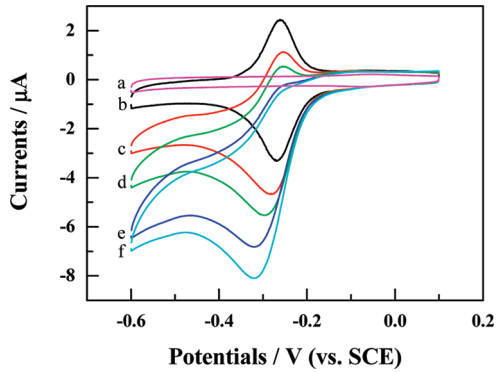

Figure 3. Voltammetric responses of the SWNT/GC (a) and Th−SWNT/GC electrodes (b−f) in N_2-saturated PBS (0.1 M, pH 7.4) in the absence (a and b) and presence of 0.1 (c), 0.2 (d), 0.4 (e), and 0.6 mM H_2O_2 (f). The scan rate is 10 mV s^{-1}.

potential range of interest (Figure 3a), whereas the Th−SWNT/GC electrode demonstrates a couple of well-defined redox peaks (Figure 3b) with the anodic (E_{pa}) and cathodic (E_{pc}) peak potential of −260 and −268 mV (at 10 mV s^{-1}), respectively, which can be ascribed to the redox reaction of thionine adsorbed on the surface of SWNTs.[52] Upon addition of 0.1 mM H_2O_2, the shape of the redox couple changes significantly characterizing with the enhancement in the cathodic peak height and the decrease in the anodic peak (Figure 3c), which is contributed from the electrocatalytic reduction of H_2O_2. The electrocatalytic currents are increased significantly by a further increase of the concentration of H_2O_2 (Figure 3d−f, 0.2−0.6 mM H_2O_2).

The controlled experimental results show that the electrocatalytic activity of the bare GC, Th/GC, and SWNT/GC electrodes toward the reduction of H_2O_2 is too low to be observed obviously (Figure 4). These results suggest that the electrocatalytic reduction of H_2O_2 presented in Figure 3c−f is resulted from the synergistic effects of thionine and SWNTs, demonstrating that Th−SWNTs may be used for a platform to sense the oxidase-based substrates (for example, UA).

Electrocatalytic Oxidation of UA at the UOx−Th−SWNT/GC Electrode. The aim of this work is to develop a biosensor for selectively analyzing the level of UA in both the physiological (serum) and endogenous (cell lysate) environment. To study the possibility of the UOx−Th−SWNT/GC electrode being used for this purpose, the voltammetric responses of the electrode in PBS with and without UA are recorded. The results are depicted in Figure 5. In the absence of UA, the cyclic voltammogram of the electrode shows characteristics of the redox reaction of thionine (Figure 5a), suggesting that the immobilization of UOx on the surface of SWNTs does not affect the electrochemical characteristics of thionine. Moreover, the response of the electrode is fairly stable since the shape and size of the redox peaks almost remain invariant even after the electrode was continuously scanned for a long time (ca. 100 cycles at 5 mV s^{-1}). This feature is important when the electrode is used as a biosensor to sense the substrate. Upon addition of 0.1 mM UA, the shape of the cyclic voltammogram of the electrode changes significantly and is characterized by a large cathodic peak at ca. −380 mV (Figure

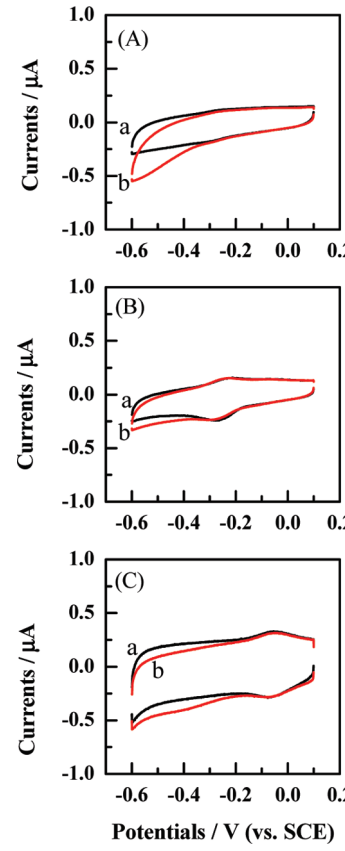

Figure 4. Voltammetric responses of the bare GC (A), Th/GC (B), and SWNT/GC electrodes (C) in N_2-saturated PBS (0.1 M, pH 7.4) with (curve b) and without (curve a) 0.5 mM H_2O_2. Scan rate: 10 mV s^{-1}.

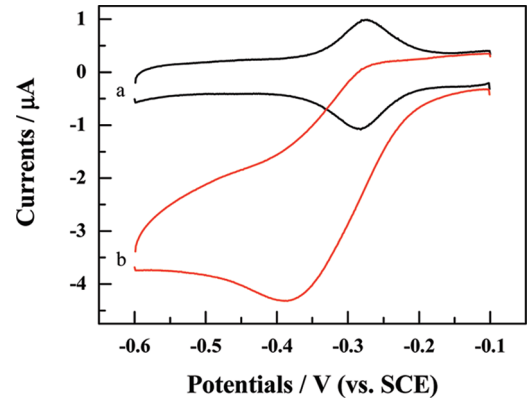

Figure 5. Cyclic voltammograms of the UOx−Th−SWNT/GC electrode in air-saturated PBS with (b) and without (a) 0.1 mM UA. The scan rate is 5 mV s^{-1}.

5b). The onset potential (ca. −150 mV) is 230 mV more positive than the reduction peak actually appears. The UOx catalyzes, in the presence of oxygen, the oxidation of UA to allantoin, producing H_2O_2 simultaneously. Therefore, the anodic peak at Figure 5b is resulted from the electrocatalytic reduction of the enzymatically generated H_2O_2. The increase of UA concentration leads to the enhancement of the cathodic current. These characteristics are the typical features of electrocatalytic reactions. Control experiments show that electrocatalytic oxidation of UA does not occur at the Th−SWNT/GC (without UOx) electrode. Moreover, the electrocatalytic oxidation of UA at the UOx/GC, UOx−Th/

(52) Meng, L.; Wu, P.; Chen, G.; Cai, C. X. *J. Electrochem. Soc.* **2008**, *155*, F231–236.

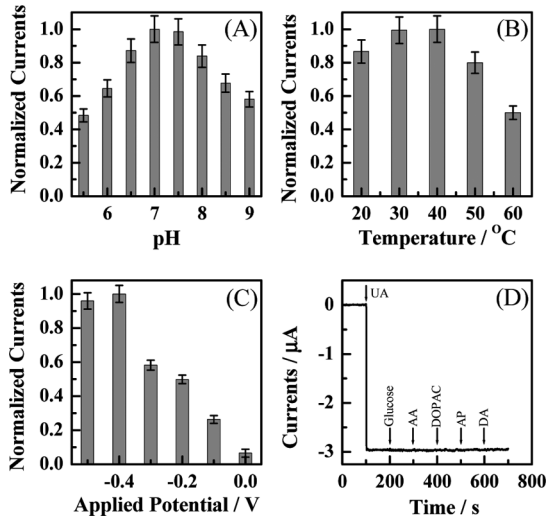

Figure 6. Dependence of the response of 0.1 mM UA at the UOx−Th−SWNT/GC electrode on the pH of the buffer (A), the temperature of the system (B), and the detection potential (C). For a better comparison, the currents are normalized by the highest response at each condition. Part D shows the selectivity profile of the electrode over interfering species of glucose (5 mM), AA (0.1 mM), AP (0.1 mM), DOPAC (0.1 mM), and DA (0.1 mM) obtained at applied potential of −400 mV. Every value is an average value of three independent measurements.

GC, and UOx−SWNT/GC electrodes can hardly be observed (not shown here). These results suggest that the UOx−Th−SWNT/GC electrode can be used as a biosensor to detect UA. The electrocatalytic processes that occurred at the electrode surface can be depicted as the following:

$$\mathrm{UA} + \mathrm{O_2} \xrightarrow{\mathrm{UOx}} \text{allantoin} + \mathrm{H_2O_2} + \mathrm{CO_2} \qquad (1)$$

$$\mathrm{H_2O_2} + \text{thionine(Red)} \rightarrow 2\mathrm{H_2O} + \text{thionine(Ox)} \qquad (2)$$

$$\text{thionine(Ox)} + \mathrm{H^+} + 2\mathrm{e} \rightarrow \text{thionine(Red)} \qquad (3)$$

The response of the biosensor usually depends on the solution pH, performance temperature, and the detection potential. This work optimized these parameters. The response was independently tested thrice for each pH, temperature, and the applied potential, and an average value was calculated.

The solution pH and temperature has significant effects on the performance of the biosensor. The response increases with the solution pH and reaches a plateau at the pH of 7.0−7.5, and then it decreases slightly with further increasing of solution pH (part A in Figure 6). The response increases slightly with the increasing of temperature and reaches a relatively stable value between the temperatures of 30−40 °C (part B in Figure 6). At higher temperature, the response decreases due to the denaturation of the enzyme. Therefore, the physiological pH and temperature (pH 7.4 and 37 °C) are chosen as the optimal condition for the UOx−Th−SWNT/GC electrode sensing UA.

The choice of the detection potential is necessary to achieve the lowest detection limit and avoid the electrochemical interfering species. The responses of 0.1 mM UA at the UOx−Th−SWNT/GC electrode at different detection potentials were recorded and

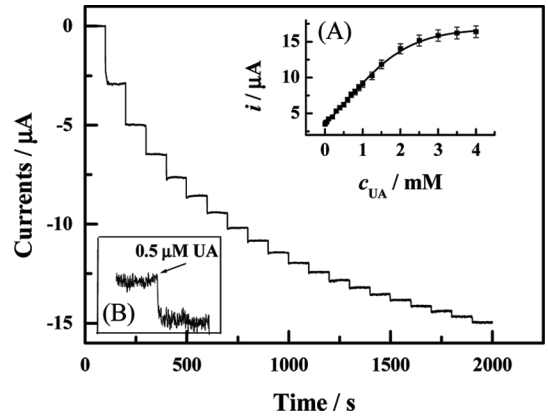

Figure 7. Amperometric responses of the UOx−Th−SWNT/GC to the successive addition of UA in PBS (0.1 M, pH 7.4) at an applied potential of −400 mV. Each addition of UA is 50 μM. The inset shows the dependence of the response of the electrode on UA concentration under the optimal condition (inset A) and the relationship of the signal-to-noise ratio at S/N of 3 (inset B).

compared. The potential range was from 0 to −500 mV with a settled interval of 100 mV. The results are presented in part C of Figure 6. Basically, the response keeps on rising when the potential is moved from 0 to −400 mV and decays slightly after that potential. Moreover, a more negative potential leads to increase in noise. Thus, a detection potential of −400 mV is selected in this work. This potential is 300, 500, 700, and 850−900 mV more negative than those used at the UA biosensors by immobilizing UOx in DTB−PET/MPx-11 film (−100 mV),[16] in Prussian blue-coated indium tin oxide substrates (100 mV),[17] on the surface of tin oxide-functionalized multiwalled carbon nanotubes (300 mV),[53] and on ZnS quantum dots (450−500 mV),[42] respectively. The low detection potential will significantly diminish the influence of those easily oxidizable species.

In real samples, there are some coexisting electroactive species such as glucose, AA, DOPAC, DA, AP, etc. that might affect the biosensor response. The selectivity and anti-interference advantages of the biosensor are demonstrated (part D in Figure 6). A well-defined UA response is observed at the biosensor, whereas relevant physiological levels of AA, DOPAC, DA, AP (0.1 mM), and glucose (5 mM) result in negligible signals. This feature is largely attributed to the use of a low operating potential in the detection. Therefore, highly selective response to UA is obtained without the use of a perm-selective membrane or enzymatic preoxidation. This is an advantage of the proposed biosensor over those reported previously. These results indicate the suitability of the proposed biosensor to practical applications.

Analytical Performances of the UOx−Th−SWNT/GC Electrode. Figure 7 depicts the typical amperometric response of the UOx−Th−SWNT/GC electrode to the successive addition of UA (50 μM for each addition) in solution at a detection potential of −400 mV. Immediately after the addition of UA, the response increases and reaches 95% of the steady-state value within ~2 s. The response time is much shorter than those obtained at other electrodes; for example, the response time is 10 and 80−100 s at the UOx−DTB−PET/MPx-11 electrode for the low (<10 μM) and high concentration of UA (~100 μM),[16] respectively, and 60 s at

(53) Zhang, F. F.; Wang, X. L.; Li, C. X.; Li, X. H.; Wan, Q.; Xian, Y. Z.; Jin, L. T.; Yamamoto, K. *Anal. Bioanal. Chem.* **2005**, *382*, 1368–1373.

polyaniline−UOx and egg shell membrane−UOx electrodes.[40] These results suggest that the UOx−Th−SWNT/GC electrode responds rapidly to the change of the substrate concentration. The electrode linearly responds to UA at lower concentration and attains saturation level at higher concentration as expected for Michaelis−Menten-type enzyme kinetics (the inset A of Figure 7). The apparent Michaelis−Menten constant (K_M^{app}) is estimated to be ~0.87 mM from the Lineweaver−Burk plot. The response displays a good linear range from 2 μM to 2 mM with a correlation coefficient of 0.998 and a slope of 6.5 ± 0.4 μA mM^{-1}. Therefore, the sensitivity is evaluated to be ~90 μA mM^{-1} cm^{-2}. The upper limit of the linear range is far beyond the physiological level (0.3−0.5 mM), suggesting that the biosensor developed here would be useful in determination of the UA concentration in physiological level. The detection limit is estimated to be ca. 0.5 ± 0.05 μM at a signal-to-noise ratio (S/N) of 3 (Figure 7, inset B), which is much lower than that obtained at a UA biosensor based on polyaniline−UOx (10 μM).[41] The linear response range is wider than those of 4 μM−0.64 mM,[40] 10 μM−0.6 mM,[41] and 5−150 μM.[16] The sensitivity is also much higher than that acquired previously (3.4 ± 0.08 μA mM^{-1} cm^{-2}).[16]

Different aspects regarding the characteristics of the biosensor are evaluated. The RSD (relative standard deviation) is ~2.4% estimated from slopes of calibration plots for 10 different and freshly prepared electrodes, revealing an acceptable repeatability in the construction of the biosensor. The assay precision of the biosensor was examined by 10 determinations at UA concentration of 0.2 mM. An RSD of ~2.8% is obtained. Also, the long-term stability of the biosensor is considered. When the electrode was not in use, it was stored in buffer at 4 °C. Its response to 0.2 mM UA was recorded at every 2 day interval. The response reveals that the electrode maintains ca. 90% of its initial current response to the UA even after 1 month. Even after the biosensor has been used for 1 week (four measurements a day), its response still remains at ca. 85% of the initial value. However, the response of the biosensor was decreased to ca. 70% of its initial one after the biosensor was used for continuous measurements for 1 month. This may be caused by the leaking of the enzyme and thionine from the surface of the electrode. Another attractive feature of the biosensor is that the response can still retain ca. 92% of its original signal even after it is under extended polarization at −400 mV for 2 h in a stirred solution of 0.2 mM UA. This means that the biosensor can be used as a stable probe for UA detection. The high stability can be attributed to the capability of the Th−SWNTs nanostructures adsorbing UOx molecules and retaining their biological activities. This improved stability may also be attributed to the special structure of the UOx−Th−SWNTs (Figure 2b), which is beneficial for the substrates getting access to the enzyme molecules. In addition, the fast diffusion of species from nanotubes may also contribute to the improvement in stability of the biosensor.

Determination of UA in Physiological Samples. To evaluate its applicability, the biosensor was used for determination of the concentration of UA in blood serum samples. Five serum samples obtained from a hospital were analyzed by using five independently prepared biosensors (one biosensor for per sample). The determined results were compared with those provided by the hospital (Table 1). It is shown that the values measured by the proposed biosensor are in good agreement with the data provided by the hospital within 5% error, demonstrating the great potential for practical application of the biosensor for the analysis of UA on physiological real clinical samples.

Table 1. Determination of UA Concentration in Serum Samples Using the Developed Method

sample no.	referenced values (mM)[a]	determined values (mM)[b]	relative deviation (%)
1	0.50 ± 0.02	0.48 ± 0.03	−4.0
2	0.46 ± 0.08	0.45 ± 0.02	4.3
3	0.43 ± 0.03	0.41 ± 0.05	−4.6
4	0.39 ± 0.06	0.40 ± 0.04	2.5
5	0.35 ± 0.02	0.36 ± 0.05	2.8

[a] Value provided by the hospital. [b] Value determined by the UOx−Th−SWNT/GC biosensor; it is an average value of the response of five measurements for each sample.

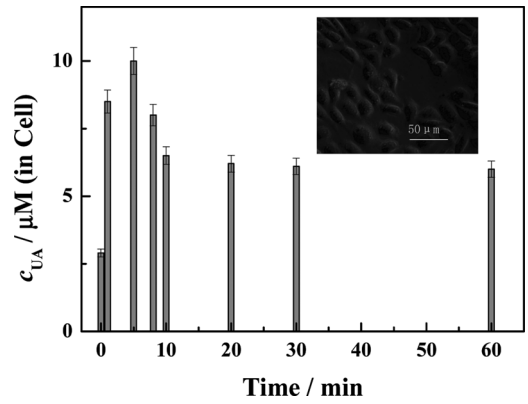

Figure 8. Time-dependent concentration of UA in HEK 293A cells after treatment with 5 mM fructose. The inset shows the image of HEK 293A cells recorded with an AxioObserver.A1 microscope (Carl Zeiss).

Determination of UA in Endogenous Samples. The developed method was also used to determine endogenous UA concentration in HEK 293A cells. The results indicated that the UA concentration in HEK 293A cell is ca. 3 μM (Figure 8), which is in agreement with that reported previously based on a liquid chromatography and tandem mass spectrometry (LC−MS/MS) method using 1,3-^{15}N-UA as the isotopically labeled internal standard.[25] The developed method was also used to measure UA endogenously in HEK 293A cells in response to fructose treatment since fructose is known to generate UA within cells as a consequence of fructose-induced ATP depletion, intracellular phosphate reduction, and stimulation of AMP deaminase.[54,55] Figure 8 depicts the time course experimental results with fructose loading. The value of UA in HEK 293A cells is significantly increased after treatment with 5 mM fructose with only 1 min, and it reaches the highest value (ca. 10 μM) at 5 min. Afterward, the concentration decreases gradually and reaches the relatively stable value (ca. 6−7 μM) at 20 min. Therefore, the proposed method should be used for studying the intracellular kinetics of UA.

To evaluate the precision of the UA concentration in HEK 293A cells detected with the developed method, the recovery measure-

(54) Hallfrisch, J. *FASEB J.* **1990**, *4*, 2652–2660.
(55) Mayes, P. A. *Am. J. Clin. Nutr.* **1993**, *58*, 754S–765S.

Table 2. Recovery Measurements of UA in HEK 293A Cells Using the Developed Method

sample no.	added amounts (μM)	measured amounts (μM)[a]	recovery (%)	RSD (%)
1	2	1.95	97.5	3.15
	3	3.05	101.6	
	6	6.22	103.7	
2	2	2.03	101.5	2.60
	3	3.12	104	
	6	5.93	98.8	
3	2	2.08	104	3.43
	3	2.92	97.3	
	6	6.12	102	

[a] Values determined by the UOx−Th−SWNT/GC electrode; it is an average value of the response of five measurements for each sample.

ments were carried out. Three intracellular samples (HEK 293A cell lysate) were prepared, and certain amounts of UA were added. The results are presented in Table 2. The average recoveries for the three different samples are 100.9%, 101.4%, and 101.1%, respectively, and the RSDs are 3.15, 2.60, and 3.43%, respectively, indicating that the developed approach has high accuracy in measuring UA concentrations in intracellular sample. These observations substantially demonstrate that the developed method represents a new biosensing platform for reliable determination of intracellular UA and could be potentially useful for further physiological and pathological studies.

CONCLUSIONS

A new amperometric UA biosensor based on the immobilization of UOx on the surface of Th−SWNT nanostructures has been developed. The biosensor exhibited a fast response, a broad linear range, a low detection limit with satisfactory stability and repeatability and would have great potential application in determination of UA concentration in both endogenous and physiological samples. The fabrication method of the biosensor has many advantages such as ease of fabrication, enhanced electrocatalysis, efficiently preserving the activity of enzyme molecules, and effective discrimination to the common interfering species.

ACKNOWLEDGMENT

This work is supported by the National Natural Science Foundation of China (20673057, 20773067, 20833006, and 20905036), the Program for New Century Excellent Talents in University (NET-06-0508), and the Foundation of the Jiangsu Education Committee (09KJA150001 and 09KJB150006).

Received for review December 11, 2009. Accepted February 10, 2010.

AC9028246